POAC'15
Trondheim, Norway

Proceedings of the 23rd International Conference on
Port and Ocean Engineering under Arctic Conditions
June 14-18, 2015
Trondheim, Norway

A CONCEPT DESIGN FOR A MESO-SCALE FLOATER TO MEASURE DOWNWARD BENDING FAILURE ICE LOADS

Marnix van den Berg [1], Sveinung Løset [1]
[1] Sustainable Arctic Marine and Coastal Technology (SAMCoT), Centre for Research-based Innovation (CRI), Norwegian University of Science and Technology, Trondheim, Norway

ABSTRACT

When designing a floating structure for regions where sea ice may occur, it is imperative to have an accurate prediction of the ice loads. Currently there is a big difference in predicted forces between several prediction methods. There is little full-scale load data to verify existing methods. Furthermore, it is not fully clear how well small-scale ice tank experiments can be scaled to full-scale. Force measurements on a meso-scale structure could bridge the gap between small-scale measurements and full-scale data. Results could be used to verify existing load models and develop new ones.

This paper presents a concept design for a moored omnidirectional floating buoy with downward sloping sides to measure ice bending failure loads in field conditions. A numerical ice-buoy model is developed to optimise the design and to examine buoy behaviour when loaded by ice. The results show that for a shallow draft design a minimum waterline diameter of 8 m is needed to have ice bending failure up to an ice thickness of 0.6 m. In thicker ice, the buoy will incline too much and the ice will no longer fail in bending. To ensure the safety of the buoy design, a load limiting mechanics based on submersion of the buoy is proposed. This can limit the ice loads in ice thicker than 0.6 m.

INTRODUCTION

Currently there is little full-scale data available regarding the loading by level ice on moored floating structures. The only full-scale data set known to the authors comes from the Kulluk drilling vessel and is described in Wright (2000). Ice tank tests on moored floaters have been done by Bruun et al. (2011), Dalane et al. (2014), Jensen et al. (2008) and Løset et al. (1998). Because of the scaling laws applied in ice tank tests, the stiffness and strength of the ice is usually much lower than that of real sea ice. The similitude of ice tank tests to full-scale is debated. Palmer and Dempsey (2009) argue that the fracture behaviour changes by scaling the ice strength and stiffness. Other factors that might change are the load distribution on the hull and the transition between inertia- resonant and stiffness dominated interaction regimes. Meso-scale experiments could provide information on the effect of scale in floater-ice interaction. It could bridge the gap between lab-scale and full-scale. An understanding of the differences between ice tank experiments on moored floaters and full-scale is imperative for the correct interpretation of ice tank test data and for the development and verification of ice loading models.

The main purpose of a meso-scale ice measurement buoy would be to provide ice loading data that can be used to develop new load determination methods and to verify existing design calculations. Designing such a buoy is challenging.
As mentioned above, the main reason to deploy a meso-scale buoy is that it is currently unclear how to properly calculate ice loads on a moored floating structure. Nevertheless, these ice loads must be calculated in order to make a reliable buoy design. Due to its size, a meso-scale buoy would need to be deployed in field conditions. This poses additional challenges, since the ice conditions cannot be controlled. Therefore the buoy would need to be able to withstand severe ice conditions relative to its size. Existing ice load calculation procedures do no longer apply in this case due to the large displacement and rotation of the buoy.

An earlier study with a moored floater in field conditions is described by Toyama and Yashima (1985). In their experiments, a moored conical buoy with a top diameter of 3.3 m was deployed in a lagoon. It was loaded by saline ice with a thickness of 5.1 cm. The loading model as proposed by Toyama and Yashima predicted the ice loads fairly well. However, for such thin ice the crystalline structure of the ice might be significantly different from that of thicker ice. This might influence the failure behaviour. The crystalline structure of the ice is not described in the paper of Toyama and Yashima. A concept design for a meso-scale floater was proposed before by Bruun and Gürtner (2012). Bruun and Gürtner proposed a SPAR-type design with a waterline diameter of 9 m and a draft of 63.6 m.

The concept presented in this paper is aimed at minimizing the size of the meso-scale buoy, while maximizing the range of ice conditions in which useful measurements can be obtained. The concept is designed such that ice bending failure will occur up to an ice thickness of 0.6 m. A shallow draft design is chosen because it better resembles existing floaters and floater concepts. To limit the ice loads in more severe ice conditions, a load limiting mechanism is proposed based on submersion of the buoy. In order to determine the ice loads and corresponding buoy behaviour, a numerical model of the buoy-ice system was developed.

Section 2 describes the numerical model that was developed and used to determine the ice loads and buoy behaviour. Section 3 presents the concept buoy and mooring design. Section 4 evaluates the buoy behaviour in various cases of interest. Section 5 discusses the possible uses and limitations of data acquired with a meso-scale buoy, and it elaborates on the limitations of the numerical buoy-ice model that was used in the design. Finally, Section 6 concludes the paper.

BUOY-ICE MODEL

A new buoy-ice model is developed for the concept design of the meso-scale buoy because existing ice loading models are not capable of capturing the highly non-linear behaviour that occurs in the limit case. The following section will explain the buoy-ice loading model and will attempt to place the model in the context of existing ice loading models. Load models differ in the following ways;

- Whether they predict a maximum load or a temporal load signal.
- Whether they assume simultaneous failure or non-simultaneous failure.
- Whether they use analytical or numerical methods.
- How they include the broken ice, cracking, plate vs. beam, 2D vs. 3D etc.

Early analytical methods include Ralston (1977), and Croasdale and Cammaert (1994). These methods are also adopted in the ISO19906 code (2010). Toyama and Yashima (1985) were the first to include the influence of floater dynamics in their ice load calculations.
Wille et al. (2011) compared the results from a dynamic ice loading model to ice tank model tests in order to study the applicability of a beam model for the ice. A similar model was used by Shkhinek et al. (2004) to model level ice action on floating anchored structure concepts for the Shtokman field. Models by Lubbad and Løset (2011) and Aksnes (2011) model the non-simultaneous failure of the ice. A notable finding in the paper of Lubbad and Løset is that the transportation of broken ice pieces along the hull gives a significant contribution to the total ice resistance of icebreakers. The model described in Lu et al. (2014) studies the ice failure, rotation and ventilation phases in detail and gives a load signal in the time domain.

Model overview

The load model used in the design of the buoy considers the ice as four wedge shaped Euler-Bernoulli beams on a Winkler foundation. The buoy is modelled by dividing the hull into a large number of small panels. The mooring lines are modelled using the catenary equation. This model is unique in that it combines a dynamic Finite Element ice model with a dynamic buoy and a non-linear catenary mooring line model. The model output gives a temporal ice load and buoy movement signal. An overview of the model is shown in Figure 1-2.

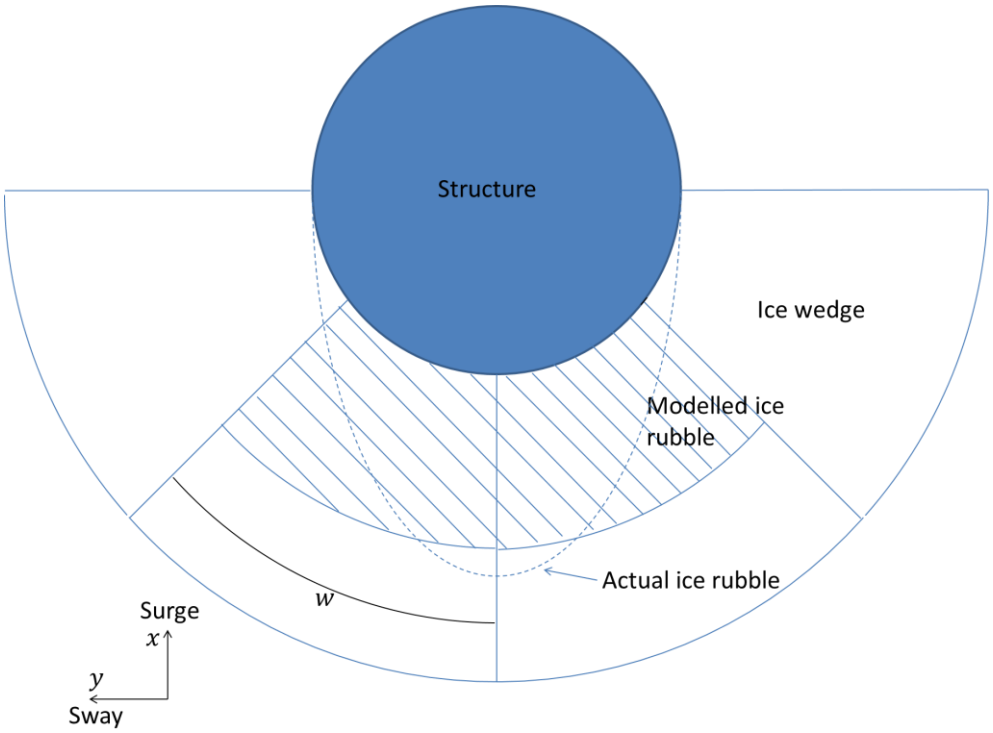

Figure 1. Top view of buoy and ice model. The ice is modelled as four wedge-shapes Euler-Bernoulli beams.

Ice rubble is modelled as an upward force on the middle two ice beams. The thickness of the accumulated rubble is assumed to be at maximum three times the ice thickness and cannot extend below the underside of the buoy. The upward rubble force is assumed to extend away from the structure for half the structure diameter. The ice is supported by a Winkler foundation and is simply supported 50 m away from the structure. For the ice thickness range of interest, this is sufficiently far not to influence the failure behaviour of the ice. The contact between the buoy and the ice is modelled as a stiff spring.

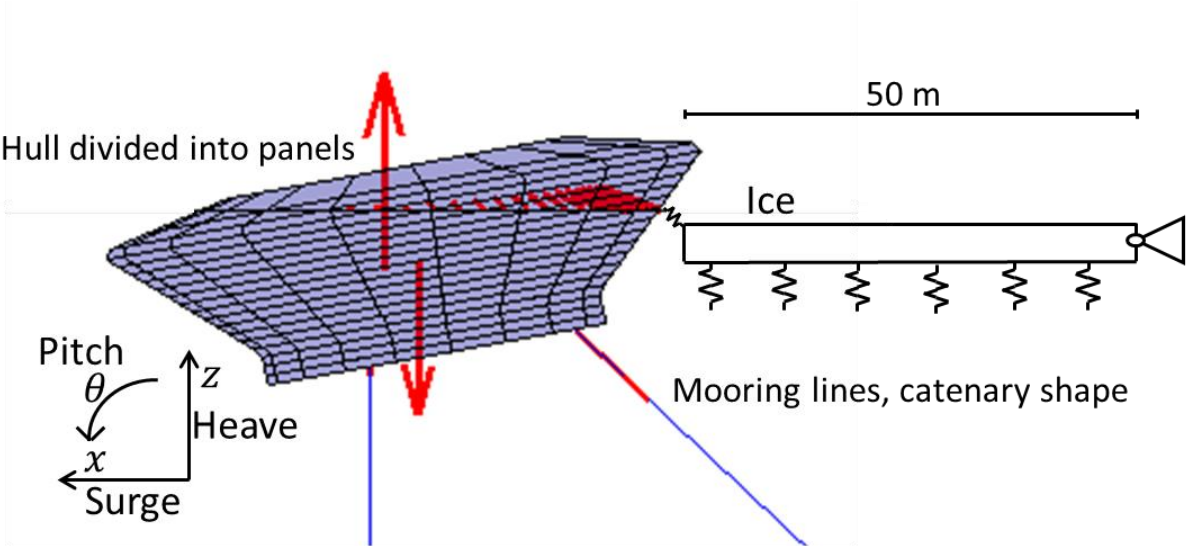

Figure 2. Side view of ice model.

The buoy is modelled by dividing the hull surface into a large number of panels. This method was chosen because it can provide the correct hydromechanic restoring forces in any buoy orientation. This is needed because the buoy might show high pitch rotation in the limit case. The bottom might leave the water and the top might be submerged. Important model parameters are given in Table 1.

Table 1. Model parameters.

Parameter	Symbol	Value
Young's modulus ice	E	5.00 (GPa)
Flexural failure stress ice	σ_f	350 (kPa)
Density water	P_w	1025 (kg/m^3)
Density ice	P_i	900 (kg/m^3)
Ice-hull friction coefficient	μ	0.2
Ice thickness	h	Variable (m)
Surge, sway, heave	x,y,z	Variable (m)
Roll, pitch, yaw	ϕ,θ,ψ	Variable (°)

Mooring system model

The mooring restoring force in each timestep is calculated by solving the catenary equation for each section of mooring line. An overview of all variables is shown in Figure 3.

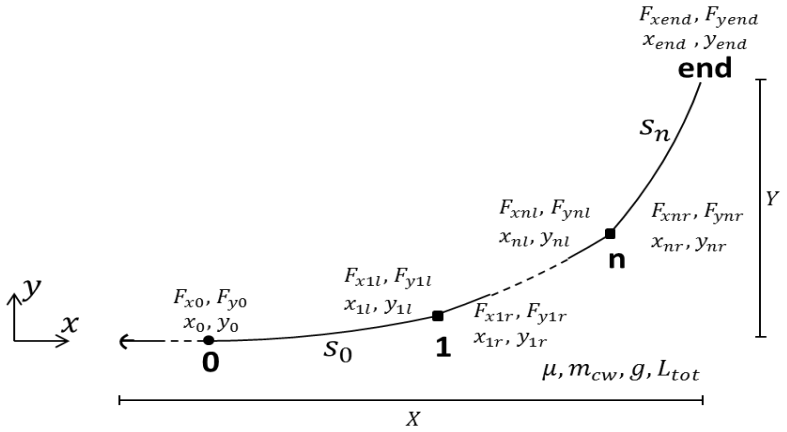

Figure 3. Variables in the catenary mooring line model.

Point **0** is where the mooring line touches the seafloor. At this point the vertical mooring force $F_{y0} = 0$. The horizontal mooring force is assumed constant over the mooring line; $F_{x0} = F_{x1} \ldots F_{xend}$. Points **1** ... **n** indicate the locations of the clump weights, in which *n* is the number of clump weights lifted from the seafloor. Point **end** indicates the connection point of the mooring line to the buoy. The variables used in the calculation are explained in Table 2.

Table 2. Explanation of mooring line variables.

Variable	Explanation
X, Y	Coordinate of end point of mooring. This is where the mooring line is attached to the buoy. In local coordinate system with origin at anchor point and *x*-axis parallel to horizontal component of mooring line.
μ_{sub}	Submerged weight per unit length
m_{cw}	Submerged weight of clump weights
g	Gravity acceleration
L_{tot}	Total length of mooring line
s_n	Length of mooring line section n
F_{xnl}, F_{ynl}	Horizontal and vertical mooring force at left side of point n
F_{xnr}, F_{ynr}	Horizontal and vertical mooring force at right side of point n
x_{nl}, y_{nl} / x_{nr}, y_{nr}	x *and* y coordinate in local coordinate system

Using basic mathematics, the following identities can be derived for a catenary line (described, among others, by Weisstein, 2015);

$$a = \frac{F_x}{\mu \cdot g} \tag{1}$$

$$x = \sinh^{-1}\left(\frac{F_y}{F_x}\right) \cdot a \tag{2}$$

$$y = a \cdot \cosh\left(\frac{x}{a}\right) \tag{3}$$

Note that the x and y values in the above formulas are not the x and y coordinates in the coordinate system as given in the above figure. Rather, the difference between the left x coordinate at point **n** and the right x coordinate a point $\mathbf{n-1}$ is the horizontal distance between point **n** and point $\mathbf{n-1}$. The horizontal and vertical coordinates of the mooring attachment point can be calculated as follows;

$$X = (x_{end} - x_{nr}) + (x_{nl} - x_{n-1r}) + \cdots + (x_{1l} - x_0) + (L_{tot} - s_n - \cdots - s_0) \tag{4}$$

$$Y = (y_{end} - y_{nr}) + (y_{nl} - y_{n-1r}) + \cdots + (y_{1l} - y_0) \tag{5}$$

The only unknowns in these equations are the horizontal mooring force F_x and the mooring line length between the last lifted clump weight and the touchdown point s_0. This gives a system of 2 equations with 2 unknowns, hence a solution can be found. The solution is obtained using the bisection method.

Ice model

The ice is modelled as four wedge shaped Euler-Bernoulli beams on a Winkler foundation. This can be seen as a hybrid form between a simple beam model and a full plate model. Cracks in the ice plate are assumed to have already formed, giving the four wedge shaped beams. In the initial condition the model assumes simultaneous contact between the ice and the structure. This assumption gives a conservative force prediction.

In order to verify the dynamic FEM wedge on elastic foundation model, its solution is compared to the analytical solution for a static case. The displacement and vertical load at the moment of failure is compared. The solution for a static wedge on elastic foundation is described in Nevel (1958, 1961). The wedge parameters as defined by Nevel are given in Table 3. The loading case that is used for verification is shown in Figure 4.

Table 3: Wedge parameters.

Variable	Explanation
x	Distance along the wedge, 0 at (imaginary) tip
l	$\sqrt[4]{\frac{Eh^3}{12k}}$ = characteristic length
χ	$\frac{x}{l}$ = non-dimensional distance along wedge
E	Young's modulus
k	Foundation stiffness
h	Ice thickness
b_0	Width of the wedge at $x = 1$
r	Waterline radius of buoy
τ	$\tau = \frac{r}{l}$ =Loading point of wedge, in non-dimensional distance
F_v	Vertical load at ice-structure interface

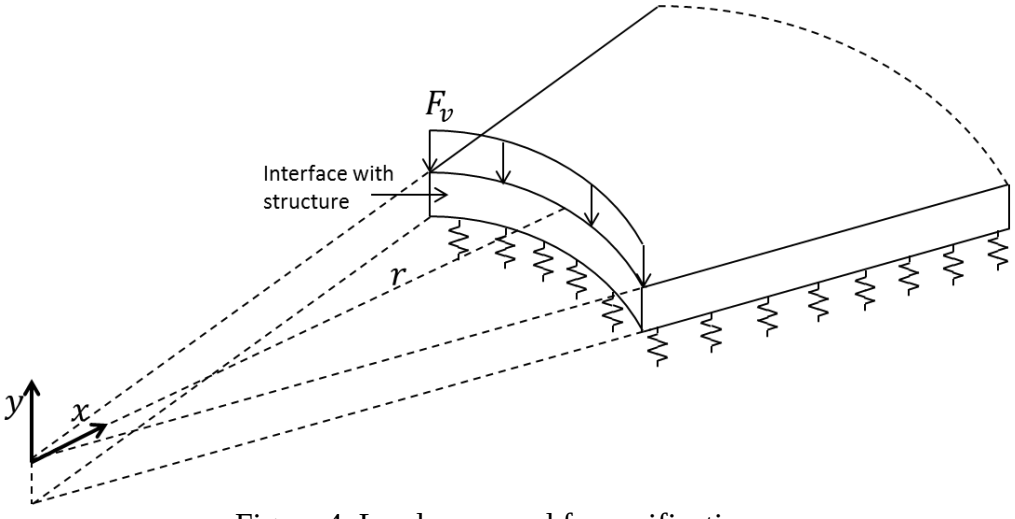

Figure 4. Load case used for verification.

Nevel formulates the solution of a wedge-shaped beam without distributed load as;

$$y = [aDn_2(\chi) + bDn_3(\chi)] \quad (6)$$

In which a and b are constants to be determined based on the boundary conditions, and Dn_2 and Dn_3 are functions of χ. The definition of Dn_2 and Dn_3 can be found in Nevel (1961). Because the displacement y in the above formula is described in terms of the non-dimensional distance χ, the moment and shear force formulations become;

$$M = \frac{EI}{l^2} y'' \tag{7}$$

$$V = \frac{b_0 h^3 E}{12 l^2} \cdot y'' + \frac{EI}{l^3} \cdot y''' \tag{8}$$

The constants a and b are computed by solving the following system of equations:

$$\begin{bmatrix} \frac{EI(\tau)}{l^2} Dn_2''(\tau) & \frac{EI(\tau)}{l^2} Dn_3''(\tau) \\ \frac{b_0 h^3 E}{12 l^2} \cdot Dn_2''(\tau) + \frac{EI}{l^3} \cdot Dn_2'''(\tau) & \frac{b_0 h^3 E}{12 l^2} \cdot Dn_3''(\tau) + \frac{EI}{l^3} \cdot Dn_3'''(\tau) \end{bmatrix} \begin{bmatrix} a \\ b \end{bmatrix} = \begin{bmatrix} 0 \\ F_v \end{bmatrix} \tag{9}$$

With a and b determined, the full analytical solution is known. The solution is compared to results from the FEM implementation. As can be seen in Figure 5, the FEM implementation predicts the same deformed shape as the analytical solution. This is as expected. The predicted failure load is 1.5% higher in the FEM model, most likely due to the grid size used. Given the inhomogeneous nature of ice, this difference is considered acceptable.

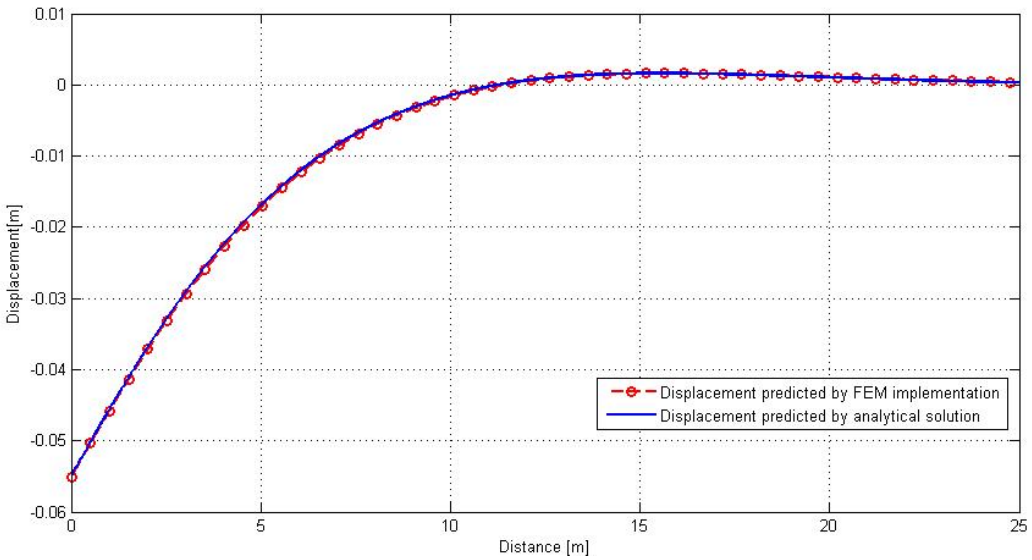

Figure 5. Displacement predicted by analytical solution compared with FEM results.

Comparison to existing models

As model verification, the limit ice loads predicted by the current model are compared to limit loads predicted by two analytical methods that are proposed in the ISO code (ISO/FDIS 19906, 2010). The model predicts peak ice loads that are lower than the loads predicted by Ralston's method (Ralston, 1977) and higher than the loads predicted by Croasdale's method (Croasdale and Cammaert, 1994). The comparison is shown in Figure 6.

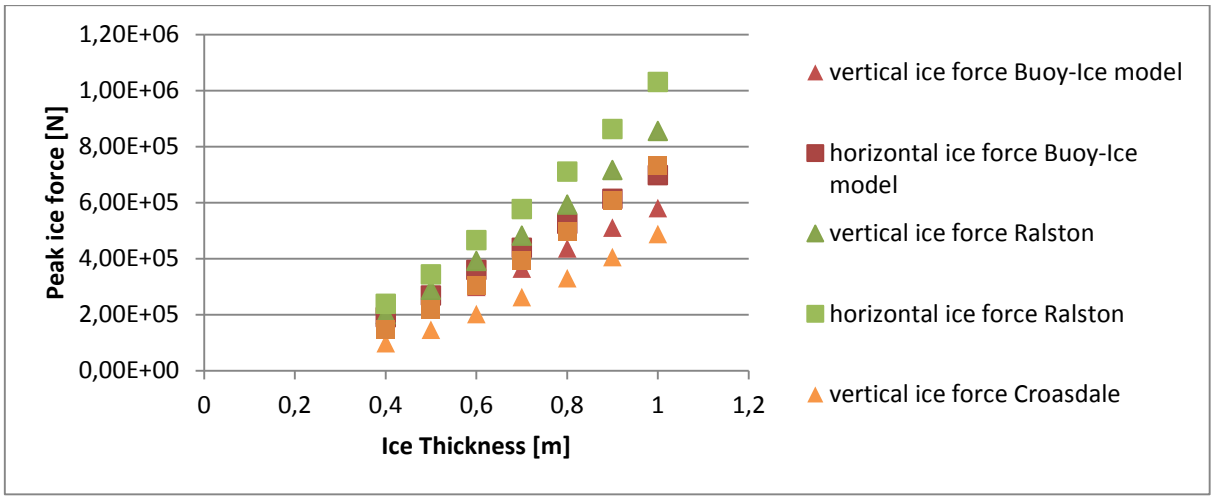

Figure 6. Comparison between the developed ice loading model and two commonly used ice load calculation methods.

For this comparison the buoy was assumed fixed, since the methods used for comparison are developed for fixed structures. Ralston's method gives a higher load prediction because this method assumes that radial cracks are formed simultaneously with circumferential cracks. The differences between the current method and Croasdale's method mostly occur because Croasdale's method does not take the curvature of the waterline into account.

BUOY DESIGN

The concept design presented in this paper is aimed at minimizing the size of the meso-scale buoy, while maximizing the range of ice conditions in which useful measurements can be obtained. Useful measurements can be obtained as long as the ice fails in downward bending. The buoy concept is designed such that ice bending failure will occur up to an ice thickness of 0.6 m. This is assumed as the limit ice thickness for locally formed ice at the west coast of Spitsbergen. Unfortunately, no measurements of ice thickness on ice floes in this location are known to the authors. The choice of 0.6 m was made in consultation with experts on the ice conditions around the Svalbard Archipelago. However, 0.6 m is not the maximum ice thickness in this region; ice drifting in from the northeast can be thicker than 0.6 m. A load limiting mechanism based on submersion of the buoy is proposed to limit the ice loads in conditions more severe than 0.6 m level ice.

There is chosen for a shallow draft design because it will be easier to install and can be installed in more shallow waters, which limits the cost of the mooring system. It also shows a better resemblance with existing full-scale structures and structure concepts. The minimum needed waterline diameter to get ice bending failure up to an ice thickness of 0.6 m is in the order of 8 m. The reason for this is the needed pitch stability. As the buoy pitches, the waterline angle increases, which increases the horizontal ice load component at the moment of ice failure. This is a self-enforcing process; the ice load increases the pitch inclination, and the pitch inclination increases the horizontal ice load where failure occurs. It can lead to an unstable situation, in which the ice no longer fails in bending.

The optimal draft of the buoy is influenced by several factors. When the mooring lines extend from the bottom of the buoy, it benefits the stability when the draft of the floater is as low as possible.

This minimizes the overturning moment caused by the horizontal component of the mooring loads. Other factors influencing the draft are the needed buoyancy and the height of the conical section needed to ensure bending failure in pitched conditions. Given the design considerations mentioned above, a concept buoy design was made. It is shown in Figure 7-8 .

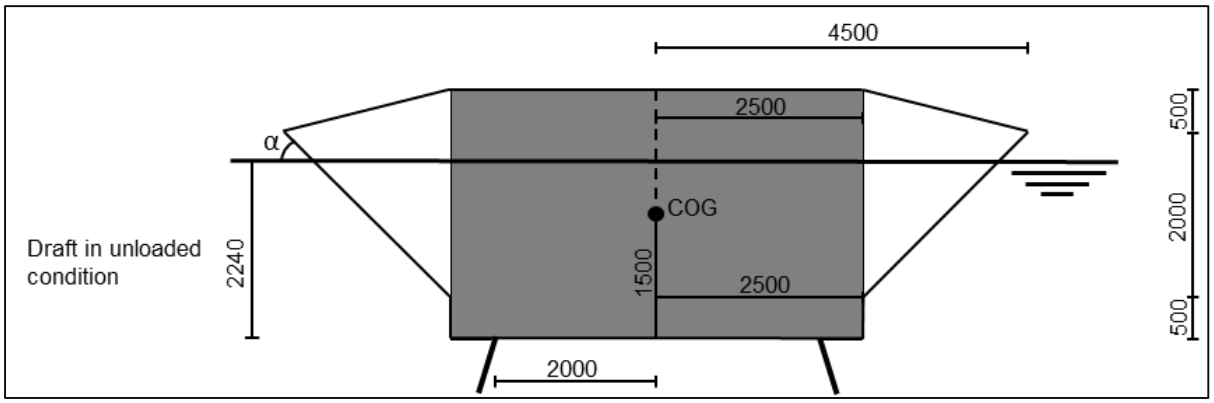

Figure 7. Concept buoy design. α = 45° (units in mm).

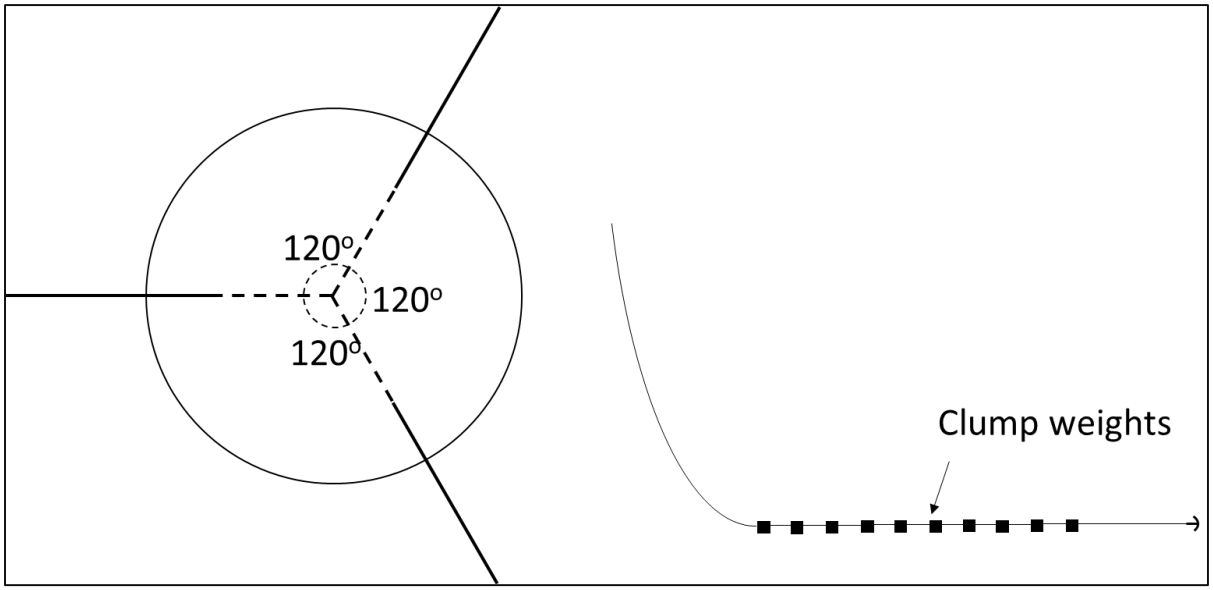

Figure 8. Sketch of concept mooring system design.

The vertical edge underneath the sloping waterline serves to deflect the broken ice. An outward sloping ice deflection skirt was considered, but was excluded from the concept design because it might prevent proper rubble clearance. A three-line mooring system is proposed. The clump weights on the mooring line cause a rapid increase of the vertical mooring load when the buoy is loaded by ice. This will cause the buoy to submerge when ice loads get too severe. The mooring system is designed for a water depth of 30 m. The total length of each mooring line is 72 m. This mooring system can easily be adapted to shallower or slightly deeper water. In much deeper water the weight of the mooring chains becomes an issue and buoyancy needs to be added either on the buoy or on the mooring chains.

BUOY BEHAVIOUR

The buoy-ice model predicts a really strong influence of pitch motion on the ice failure load. This is supported by results of ice tank experiments described in Dalane (2014).
The most interesting interaction regimes are when a geometrically scaled situation occurs and when the ice thickness approaches or exceeds the limit thickness where bending failure will occur. Both situations are discussed in this section.

With a waterline diameter of 8 m, a geometrically scaled situation approximately occurs at an ice thickness of 10-20 cm. This corresponds to a full-scale floater the size of the Kulluk (waterline diameter of 70-81 m) loaded by level ice with a thickness between 1 and 2 m. Interestingly, the ice-buoy model predicts an alternation between stiffness dominated ice failure and inertia dominated ice failure. This is shown in Figure 9. The pitch inclination θ at the moment of stiffness dominated failure is 2.6°.

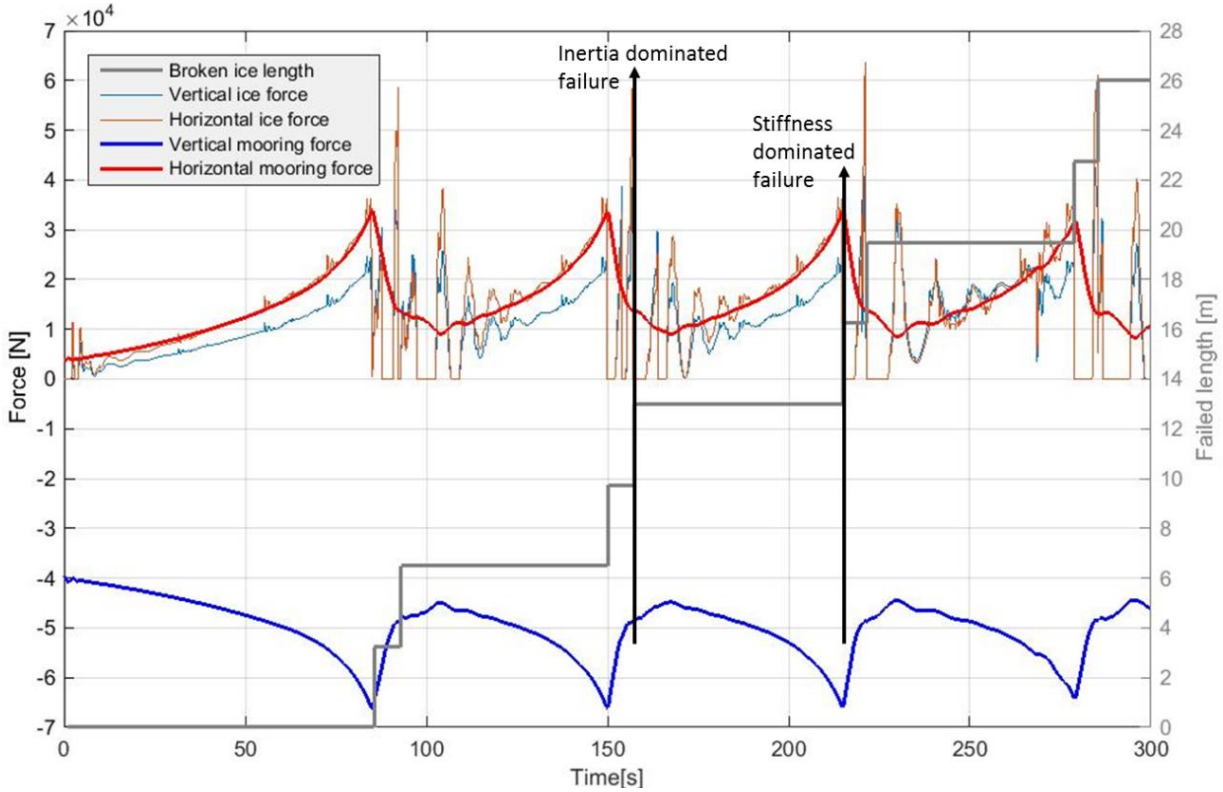

Figure 9. Ice loads, mooring loads and failed ice length in the time domain for a floater loaded by 0.2 m level ice and an ice velocity of 0.1 m/s.

With the buoy design as presented in Section 3, the ice fails in bending up to an ice thickness of 0.6 m. The buoy position right before ice failure is shown in Figure 10. The buoy has a pitch rotation θ of 16.2°, giving it a waterline angle $(\alpha + \theta)$ of 61.2°.

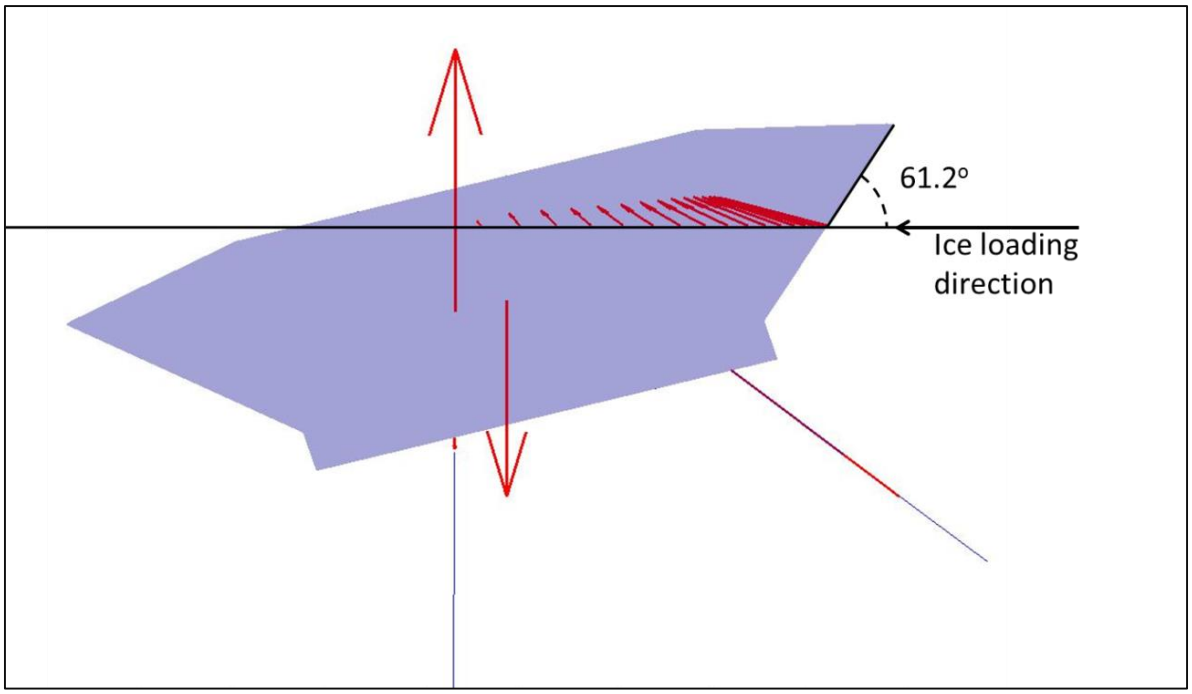

Figure 10. Buoy position right before ice failure, ice thickness h of 0.6 m and ice velocity of 0.1 m/s.

To limit the ice loads in ice conditions exceeding 0.6 m level ice, a load limiting mechanism relying on submersion of the buoy is proposed. It is based on a rapid increase of vertical mooring loads as the horizontal ice load increases, causing the buoy to submerge.

Figure 11 shows the ice and mooring loads at the moment of ice failure. When the ice fails in bending, the vertical ice load increases linearly with the ice thickness. This is in accordance with what can be expected. The horizontal ice load increases much more rapidly, due to the change in inclination of the waterline. When the ice is thicker than 0.6 m, it does no longer fail in bending. The buoy inclines too much for bending failure to occur. The horizontal ice load and mooring load increase to the point where the vertical mooring load becomes sufficiently high to submerge the buoy.

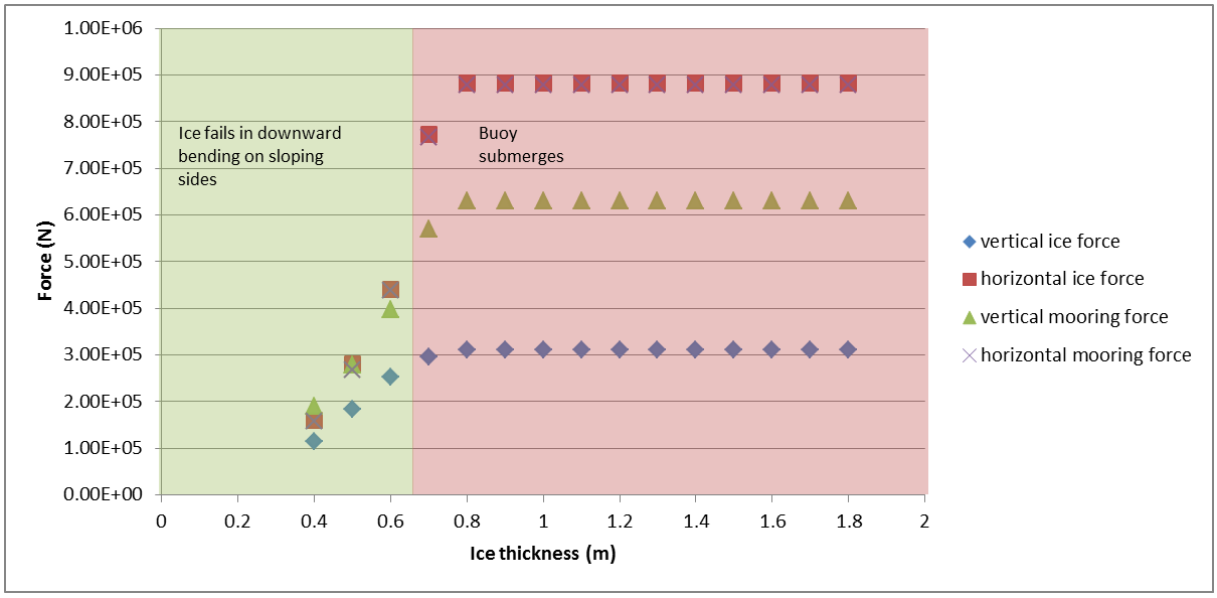

Figure 11. Ice and mooring loads at the moment of ice failure vs. ice thickness.

DISCUSSION

The behaviour of a meso-scale buoy will be inherently different from a full-scale buoy with similar geometry. This is because the ice strength is not scaled. In ice tank tests, Froude scaling and Cauchy scaling is usually applied. From this follows that the Young's modulus and flexural strength of the ice must be scaled with geometry. Due to its size, a meso-scale buoy would need to be deployed in a natural environment. Therefore it would not be possible to maintain Froude and Chauchy scaling. A geometrically scaled situation would probably occur in some ice-buoy interactions. When assuming a geometrically scaled situation, the following challenges appear;

- Ice load scales with $\lambda^{2.17}$, while buoyancy scales with λ^3. Because the weight of the mooring system is dependent on the ice load, the mooring weight can become problematic as the buoy size decreases.
- The overturning moment of the ice loads scales with $\lambda^{3.17}$, while the righting moment scales with λ^4. This has as a consequence that in a geometrically scaled situation the buoy will show a much higher pitch than would occur in full-scale.

Because of the above, the data acquired from a meso-scale buoy cannot be directly translated to an equivalent full-scale case. It will however provide useful information for the development of loading models that cannot be acquired in ice tank tests. One can think of the following aspects;

- Fracture and failure behaviour of natural sea ice.
- Load distribution on the hull; simultaneous vs. non-simultaneous failure.
- The transition between inertia dominated, resonant, or stiffness dominated interaction regimes.

These are all things that can be influenced by scale and by ice properties like stiffness and fracture toughness. The authors believe that information acquired from a meso-scale buoy can provide key information for the development of ice loading models and for the interpretation of ice tank test data.

The buoy-ice model used in the design of the buoy is not considered valid in highly dynamic situations, such as loading by fast moving ice (velocity above 0.2 m/s) or the behaviour of the buoy after ice failure. The dynamic model parameters, such as hydrodynamic damping and added mass of the buoy, as well as the contact model between the ice and the buoy, are considered too simplistic for that. However, the maximum mooring load is expected to occur in a stiffness dominated regime, for which the model should work correctly.

Another limitation of the model is the way in which broken ice wedges and rubble are included. The model is more simplistic in this aspect than other existing models. There are two arguments to justify the simplistic rubble assumptions;

- Due to the small size of the buoy, the rubble will flow around relatively easy compared to a full-scale case, which reduces the importance of a rubble model.
- The load associated with rotating the broken ice pieces and rubble is most important after the ice fails, and not when the peak load occurs. Therefore the peak load will not be influenced much by a more sophisticated rubble model.

Given the above limitations, some remarks need to be made regarding the model results presented in Section 4. The inertia dominated failure, as is predicted to occur in 0.2 m level ice, is a strongly dynamic phenomenon. Therefore the model predictions for this regime might be different from what could occur in reality. However, this will not influence the buoy design because the highest mooring loads occur in the stiffness dominated regime.

CONCLUSIONS

In this paper a concept design for a meso-scale buoy is presented. For a shallow draft design, a minimum waterline diameter of 8 m is needed to ensure ice bending failure up to an ice thickness of 0.6 m. This is because of the needed pitch stability. In order to limit the ice loads in thicker ice, a load limiting mechanism is proposed based on submersion of the buoy. Data obtained from a meso-scale buoy in field ice conditions can supplement existing ice tank measurements by giving information about the effect of scale and ice properties on the following aspects;

- Force distribution along the waterline. Simultaneous vs. non-simultaneous failure.
- The transition between inertia dominated, resonant, or stiffness dominated interaction regimes.
- The failure behaviour of the ice, must notably the formation of cracks and fracture.

The numerical ice-buoy model that was developed for calibration of the buoy design predicts a large influence of pitch on the ice failure load. Due to the fact that the ice force cannot be scaled in field conditions, the results obtained from the buoy cannot be directly translated to a full-scale case. The data obtained can however be used to verify and develop numerical load prediction models for floater-ice interaction.

ACKNOWLEDGEMENTS

The authors would like to acknowledge the support from the SAMCoT CRI through the Research Council of Norway and all of the SAMCoT Parties. We also want to thank Professor R. Lubbad for his help with the analytical derivation of the wedge shaped beam on an elastic foundation.

REFERENCES

Aksnes, V., 2011. A panel method for modelling level ice actions on moored ships. Part 1: Local ice force formulation. Cold Reg. Sci. Technol. 65, 128–136. doi:10.1016/j.coldregions.2010.10.003

Bruun, P.K., Gürtner, A., 2012. Feasibility study of an unmanned floating moored buoy located in the Svalbard archipelago for monitoring of ice induced responses and ice conditions simultaneously. Proc. Twenty-second Int. Offshore Polar Eng. Conf. 4, Rhodes, Greece. pp 1338–1347.

Bruun, P.K., Løset, S., Gürtner, A., Kuiper, G., Kokkinis, T., Arild, S., Hannus, H., 2011. Ice Model Testing of Structures With a Downward Breaking Cone, in: Proceedings of the ASME 2011 30th International Conference on Ocean, Offshore and Arctic Engineering, Rotterdam, The Netherlands. pp. 911-925.

Croasdale, R.K., Cammaert, A.B., 1994. An Improved Method for the Calculation of Ice Loads on Sloping Structures in First-Year Ice. Power Technol. Eng. ??Formerly Hydrotechnical Constr. 28, pp. 174–179.
Dalane, O., 2014. Influence of pitch motion on level ice actions. Cold Reg. Sci. Technol. 108, 18–27. doi:10.1016/j.coldregions.2014.08.011
Dalane, O., Løset, S., Hilden, T.E., Gudmestad, O.T., Amdahl, J., Fjell, K.H., 2014. Ice tank testing of a surface buoy for arctic conditions, in: Proceedings of the ASME 27th International Conference on Ocean, Offshore and Arctic Engineering. Estoril, Portugal.
ISO/FDIS 19906, 2010. Petroleum and natural gas industries – Arctic offshore structures, ISO TC 67/SC 7. Final Draft International Standard, International Standardization organization, Geneva, Switzerland, n.d.
Jensen, A., Bonnemaire, B., Løset, S., Breivik, K.G., Evers, K.U., Ravndal, O., Vegard, A., Lundamo, T., Lønøy, C., 2008. First Ice Model testing of the Arctic Tandem Offloading Terminal, in: 19th IAHR International Symposium on Ice. Vabcouver, British Columbia, Canada, pp. 833–847.
Lu, W., Lubbad, R., Høyland, K., Løset, S., 2014. Physical model and theoretical model study of level ice and wide sloping structure interactions. Cold Reg. Sci. Technol. 101, 40–72. doi:10.1016/j.coldregions.2014.01.007
Lubbad, R., Løset, S., 2011. A numerical model for real-time simulation of ship–ice interaction. Cold Reg. Sci. Technol. 65, 111–127. doi:10.1016/j.coldregions.2010.09.004
Løset, S., Kanestrøm, Ø., Pytte, T., 1998. Model tests of a submerged turret loading concept in level ice, broken ice and pressure ridges. Cold Reg. Sci. Technol. 27, 57–73. doi:10.1016/S0165-232X(97)00024-4
Nevel, D.E., 1958. The narrow infinite wedge on elastic foundation. Transactions of the Engineering Institute of Canada 2 (3), 132–140.
Nevel, D.E., 1961. The narrow free infinite wedge on elastic foundation. CRREL Research Report 79. 24 pp.
Palmer, A., Dempsey, J., 2009. Model Tests In Ice. Proceedings of the 20th International Conference on Port and Ocean Engineering under Arctic Conditions, Lulea, Sweden. 40
Ralston, T.D., 1977. Ice Force Design Considerations for Conical Offshore Structures, in: Proceedings of the 4th International Conference on Port and Ocean Engineering under Arctic Conditions. St. John's, Newfoundland Canada, pp. 741–752.
Shkhinek, K.N., Bolshev, A.S., Frolov, S.A., Malyutin, A.A., Chernetsov, B.A., 2004. Modeling of Level Ice Action on Floating Anchored Structure Concepts for the Shtokman Field, in: 17th International Symposium on Ice. Saint Petersburg, Russia, pp. 21–25.
Toyama, Y., Yashima, N., 1985. Dynamic Response of Moored Conical Structures to a Moving Ice Sheet, in: Proceedings of the 8th International Conference on Port and Ocean Engineering under Arctic Conditions. pp. 677–688.
Weisstein, E.W. "Catenary." From MathWorld--A Wolfram Web Resource. http://mathworld.wolfram.com/Catenary.html
Wille, S.F., Kuiper, G.L., Metrikine, A.V., 2011. On the Dynamic Interaction Between Drifting Level ice and Moored Downward Conical Structures: A Critical assessment of the Applicability of a Beam Model for Ice, in: Proceedings of the ASME 2011 30th International Conference on Oceanm Offshore and Arctic Engineering. Rotterdam, The Netherlands, pp. 991-1005.
Wright, B., 2000. Full-scale Experience with Kulluk Stationkeeping Operations in Pack Ice PERD/CHC Report 25-44.